Research Article

Journal of Environmental Nanotechnology

Evaluation of Sustainable and Renewable Agro-Waste Adsorbent for the Removal of Hexavalent Chromium from Wastewater

L. Vidhya[1*], S. J. Pradeeba[1], B. Jeyagowri[1], K. Sivakumar[2] and V. Nirmala Devi[1]

[1]Department of Chemistry, Hindusthan College of Engineering and Technology, Coimbatore, TN, India
[2]Department of Physics, Hindusthan College of Engineering and Technology, Coimbatore, TN, India
Received: 29.04.2024 Accepted: 24.05.2024 Published: 30.05.2024
*vidhuram236@gmail.com

ABSTRACT

The present research work investigates the adsorption capacity of chromium ions from wastewater by KOH-activated agro-waste *Citrus limetta* (sweet lime) peel biochar (CLPBC). This paper reports the effects of different parameters like dosage, initial concentration, and pH of the agro-waste adsorbent using KOH-activated *Citrus limetta* peel biochar. The results revealed that the sweet-lime peel biochar removed more than 99.8 % Cr (VI) at a concentration of 100 ppm, pH 7, and the time interval between 0 and 150 min. The kineticsof the Cr (VI) adsorption on *Citrus limetta* peel biochar followed the second order. The data on adsorption befittingly matched the Langmuir isotherm. Additionally, physical structural investigations such as FT-IR, SEM, EDAX, and TGA abundantly demonstrated the same, revealing distinct phases with greater numbers of pores or adsorption sites. Higher sorption capacity indicates that KOH-activated *Citrus limetta* peel biochar can be effectivelyand economically used for the treatment of Cr (VI) ion adsorption from industrial effluents.

Keywords: Chromium; Sweet-lime peel; KOH-activated *Citrus limetta*; Biochar; Isotherm and Kinetic models; FT-IR.

1. INTRODUCTION

Because of industrial operations and technological advancements, the number of heavy metals released into the environment has been steadily rising, endangering human health (Wanna and Pairat, 2009). Chromium, a priority toxic pollutant is introduced into water from tannery and electroplating industries. Chromium exists in two oxidation states: Cr (III) and Cr (VI). The hexavalent form is more toxic than the trivalent one (Vikrant Sarin and Pant, 2006; Ramzy *et al.* 2011). The hexavalent chromium is carcinogenic and mutagenic to living organisms (Dhungana and Yadav, 2009; Jabari *et al.* 2009). It is essential to recover or eliminate the chromium before disposing of the industrial waste. Chromium (VI) from wastewater can be removed by various techniques such as chemical precipitation, electrocoagulation, ion exchange, surface adsorption, and membrane filtration. The adsorption technique outperforms all other known methods in terms of cost, ease of operation, and environmental considerations when it comes to treating wastewater containing hexavalent chromium (Owlad *et al.* 2008). Owing to its low cost and energy needs, adsorption is one of the most effective methods for eliminating contaminants from wastewater (Yang *et al.* 2013). Several studies on the creation of inexpensive adsorbents and eco-friendly methods of water contamination removal have been published. Agricultural and industrial waste materials have been used and well-documented by a large number of researchers for the removalof chromium (Attia *et al.* 2010; Jeyagowri and Yamuna, 2015). Because of its higher efficiency, wider surface areas, and more developed porous structure of the resulting materials, chemical activation is more favorable than physical activation. Active functional groups and a well-developed porous structure with a predominance of micropores are produced on the surface of biochar, when the activation process using KOH as an activating agent is used. It has been demonstrated that when the amount of impregnation rises, the amount of micropores on the surface of active carbon also increases. The present paper deals with an agro-waste adsorbent that was prepared from the pyrolysis of KOH-activated *Citrus limetta* (sweet-lime) peel. Chromium (VI) was removed from the aqueous solution using batch tests, isotherm models, and kinetic studies. The effects of different factors such as pH, adsorbent dosage, and beginning chromium (VI) content, are investigated using KOH-activated *Citrus limetta* peel biochar adsorbent.

2. MATERIALS AND METHODS

2.1 Preparation of Biochar Adsorbent (CLPBC)

The peels of *Citrus limetta* were sun dried followed by drying in the hot air oven at 100 °C for 24 h. The dried material was crushed and fed into the

pyrolysis stove. The product out of pyrolysisis referred here as biochar sample, which was sieved, and their important characteristics were analyzed and used for further experimentation. The activation process was carried out to develop the porous structure of the produced biochars. Subsequently, the materials were combined with KOH at a weight ratio of 1:2 and 1:4 (biochar:KOH). They were then put into quartz boats and heated to 600 °C at a nitrogen flow rate of 20 dm^3/h in a tube furnace. The materials were submerged for two hours at 600 °C.

2.2 Characterization of KOH-activated *Citrus limetta* peel Biochar (CLPBC)

The biochar samples were stove-sieved (< 0.25 mm) and their water-holding capacity, zeta potential, and particle size were analyzed by standard methods (Shenbagavalli and Mahimairaja, 2012). Further, proximate analyses of *Citrus limetta* peel biochar adsorbent were also carried out.

2.2.1 Zeta Potential Study

To determine the surface charge of the *Citrus limetta* biochar concerning pH, zeta potential tests were conducted using a nanoparticle analyzer (Horiba Scientific Nanopartica, Japan). Biochar weighing 0.5 g was suspended in 20 mLof solutions with pH of 4, 5.5, 7, 8, and 9 and was allowed to settle for about 30 minutes. Each sample was then tested three times, with the machine taking 5 readings for each run. The output data came in the form of mobility, zeta potential and conductance.

2.2.2 Fourier Transform Infrared Spectroscopic Analysis (FT-IR)

The biochar samples before and after chromium ion biosorption were analyzed with an FT-IR (Shimadzhu Corporation (IR affinity-1) Spectrometer), under ambient conditions. FT-IR spectroscopy was used to detect the functional groups on the biochar before and after Cr (VI) sorption. Before FT-IR analysis, the biochar sample was dried at 600 °C for 24 h. The spectra were obtained in the range of 4000 to 500 cm^{-1} with a resolution of 8 cm^{-1}. The resulting spectra were used to identify the functional groups based on their characteristic absorbance peaks.

2.2.3 Scanning Electron Microscopy (SEM)

The logarithmic phase cells interaction and non-interaction were identified microscopically. A pinch of biochar powder was fixed on the 10 mm metal stub using carbon tape (Shah and Tokeer, 2013). Then, the samples were vacuum-spuned with gold in an argon environment. A potential difference of 20 kV for the tungsten filament was used in the analysis. The surface morphology of the coated sample was observed by a Quanta FEI 250 (Czechoslovakia) Scanning Electron Microscope.

2.2.4 Energy Dispersive X-ray Spectroscopy Analysis (EDAX)

The surface elemental analyses of non-interacted log phase biochar and Cr (VI) interacted log phase biochar were carried out by EDAX. The gold-sputtered samples were analyzed and the spectra were recorded using a Quanta FEI 250 (Czechoslovakia) equipment.

2.2.5 Thermogravimetric Analysis (TGA)

TGA was performed on a Netzsch TG-209 instrument. The sample was heated in a given environment (air, N_2, CO_2, He, and Ar) at a controlled rate. The proximate characteristics were recorded by TGA.

2.3 Stock Solutions and Standards

A standard stock solution of chromium (1000 mg l^{-1}) was prepared in deionized (MilliQ) water.

2.4 Batch Adsorption Experiments

The chromium concentration was determined by UV Spectrophotometer (Systronics, Canada: Model # 167) using the 1, 5-diphenylcarbazide method (Vargas *et al.*, 2012). About 0.05 g of KOH-activated *Citrus limetta* peel biochar was placed in various 250 ml Erlenmeyer flasks and 25 ml of different initial concentrations (50-250 ppm) of chromium solution was added to them. It was mixed with the help of a rotary shaker (Orbit Shaker, Taiwan) and given 150 minutes to acclimate. To reduce the impact of carbon particles on the assay, all samples were filtered before being subjected to an examination and 540 nm was maintained as the operating wavelength. The absorbance of the supernatant solution was estimated to determine the residual hexavalent chromium concentration. Runs were made in triplicate. The Cr (VI) content in the samples was recorded and calibration plots were drawn and the adsorption capacity at equilibrium was determined (Kucic *et al.* 2012). The removal percentage of hexavalent chromium was calculated for each run as follows:

$$\text{Removal percentage } (R\%) = [(C_0 - C_e)/C_0] * 100 \ldots (1)$$

where, C_0 and C_e represent the initial and final concentrations of chromium ion in aqueous solution, respectively. The concentrations of the samples were determined using a calibration graph. The adsorption capacity (q_e) for each concentration of hexavalent chromium at equilibrium was determined by,

$$q_e = [(C_0 - C_e) \times V] / M \quad \ldots\ldots\ldots\ldots (2)$$

where, V is the volume of solution (in liters) and M is the mass of the adsorbent used (in grams). After carrying out triplicate experiments for the adsorption study, the mean values were reported.

2.5 Optimized Studies of Adsorption of Cr (VI)

The best adsorption condition for optimization wasthe effect of heavy metal concentration, adsorbent dosage, pH, and contact time. By conducting numerous trials and maintaining a pH of 7 and a metal concentration of 100 mgl^{-1}, the dosage of the adsorbent was determined. In the next set of experiments, the adsorbent dosage and metal concentration were kept as 0.05 g and 100 mg, respectively. The optimization of pH was determined in the pH rangeof 2.0 - 8.0. The solution pH was adjusted using 0.5 mol l^{-1} HCl or 0.5 mol l^{-1} NaOH. The solution pH before and after interaction with a single metal ion was determined. By maintaining the adsorbent dosage at 0.1 g and pH 7, the concentration of metal ions was varied. In every trial, after adsorption, the sorbate was decanted and separated from the sorbent by centrifugation and the supernatant was analyzed for the residual metal concentration. Triplicate batch experiments were performed and average values were presented.

2.6 Adsorption Isotherm Models

Adsorption isotherms were derived from batch experiments. The adsorption isotherm models described the relationship between the adsorbate loading on the adsorbent (Q_e) and the liquid phase concentration of adsorbate (C_e) at equilibrium conditions. The adsorption isotherms were modeled using Langmuir and Freundlich isotherms to study the mode of interaction of Cr (VI) ions with biochar, when the metal solution phase and sorbent solid phase are in equilibrium. Langmuir (Equation 1), and Freundlich (Equation 2) isothermswere plotted by using standard straight-line equations and corresponding two parameters C_e and q_e for chromium ion:

$$C_e/q_e = 1/Q_0 b + C_e/Q_0 \quad \ldots\ldots\ldots\ldots (3)$$

where, q_e (mg g^{-1}) is the amount of metal adsorbed and C_e (mg l^{-1}) is the concentration at equilibrium. Q_0 and b are Langmuir constants related to adsorption capacity and energy of adsorption, respectively.

$$q_e = K_f C_e^{1/n} \quad \ldots\ldots\ldots (4)$$

K_f and n are Freundlich isotherm parameters (Bello *et al.* 2013). The Temkin isotherm assumes that the heat of adsorption of all the molecules in the layer decreases linearly with coverage due to adsorbent–adsorbate repulsions. The Temkin isotherm equation is represented by:

$$q_e = B \ln K_t + B \ln C_e \quad \ldots\ldots\ldots (5)$$

where, B = RT/b, b is the Temkin constant related to heat of sorption (J/mol), K_t is the equilibrium binding constant (l/mol) corresponding to the maximum binding energy, R is the gas constant (8.314 J/mol K), and T is the absolute temperature (K) (Erdem *et al.* 2004).

2.7 Adsorption Kinetics

The study of adsorption kinetics is significant as it provides valuable insights into the pathways and the mechanism of the process. Kinetic experiments were carried out at equilibrium conditions. To study the mechanism of sorption and potential rate-determining steps, different kinetic models have been used to test the experimental data obtained. The aqueous samples at different time intervals and the concentrations of chromium ions were determined spectrophotometrically (Demirbas *et al.* 2004; Nevine, 2008). Different models have been used to describe the metal uptake rate. Pseudo-first order (Lagergren kinetic model) and pseudo-second-order model were applied to the sorption data. The model with the highest correlation coefficient value (R^2), close to unity was considered to be the best fit.

Table 1. Physico-chemical characteristics of *Citrus limetta* peel biochar

S. No.	Characteristics of Biochar	Values
1	pH	10
2	EC	1.91 ds/m
3	Water holding capacity	224.31%
4	Moisture content	2.08%
5	Volatile content	14%
6	Fixed carbon content	70%
7	Ash Content	16%
8	Zeta potential	-7.9 mV
9	Particle size ratio	1

3. RESULTS AND DISCUSSION

3.1 Biochar Physicochemical Properties

The biochar samples were subjected to proximate analysis and the results of the moisture content and ash content were furnished (Table 1). The fixed carbon content of the sample was high, again indicative of high carbonization. The pH is high, indicating the alkalinity of the biochar. The electrical conductivity of biochar was 1.91. Zeta potential regulates every particle-

particle interaction in a suspension and is an assessment of charge stability. From Table 1, zeta potential of biochar was found to be -7.9 mV. The stability behavior of biochar was found to be incipiently unstable. If the zeta potential is low, attraction exceeds repulsion and the dispersion will break and flocculate. It was discovered that biochar has a particle size ratio of 1.00 in Table 1.

3.2 Effect of Concentration

Using 0.05 g of biochar and pH 7, the impact of the initial Cr (VI) concentration (50 to 250 mg l^{-1}) was investigated. The findings are shown in Fig. 1. As the concentration of Cr (VI) increased (from 50 to 250 mg l^{-1}), a slight decrease (0.4 to 2%) in the removal percentage was noted. The values shown are the mean from three experiments carried out by triplicate. The optimum concentration from further studies is fixed as 100 mg l^{-1}. The possibility that biochar has more active sites per ion could account for the enhanced sorption at low concentrations (100 mg l^{-1}). Higher concentrations cause the sorption process to slow down and the removal capacity decreases because of the saturation of these active sites and the steric repulsion between solute molecules. A similar pattern of Cd adsorption onto peanut husk biochar has been discovered (Babu and Gupta, 2008).

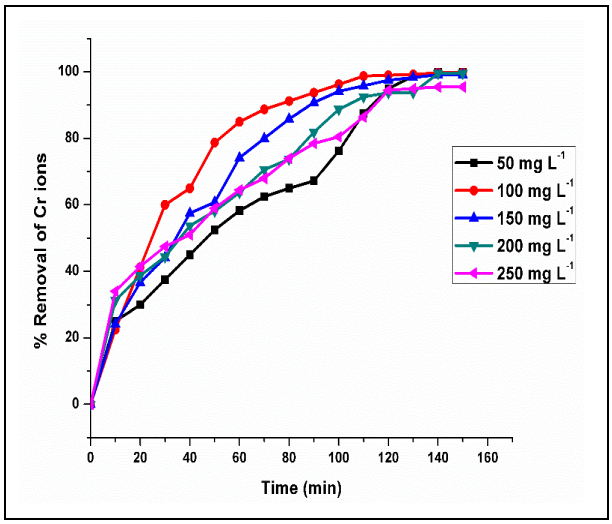

Fig .1: Effect of concentration

3.3 Effect of Adsorbent Dosage

The concentration of CLPBC has a significant impact on the sorption of metal ions from the solution because it supplies binding sites for the sorption of metal ions (Khan *et al.* 2013). The amount of adsorbent used greatly affects the adsorption process. At initial Cr (VI) concentrations of 100 mg l^{-1}, the adsorbent dosages were optimized for the removal of Cr (VI) from the solution at various time intervals ranging from 0 to 120 minutes. More surface area and more binding sites for adsorption are responsible for the dose-dependent increase in adsorption. The dosage of the adsorbent was 0.01 to 0.05 g per 100 ml, with a 0.01 g increment. Cr (VI) sorption for CLPBC reached a maximum at 99.8% and remained nearly constant for the 120-minute study period. The removal of Cr (VI) by CLPBC ranged from 99.87 to 98.8% at 120 min with various adsorbent doses of 0.01 to 0.05 g per 100 ml. The drop in adsorption capacity (Fig. 2) was basically due to the site remaining unsaturated during the adsorption process. The proportion of chromium removal increases with decreasing adsorbent dosage levels. The number of binding sites accessible for adsorption is determined by the amount of adsorbent added to the solution. (Pradeeba and Sampath, 2019). The values shown are the mean from three experiments carried out in triplicate.

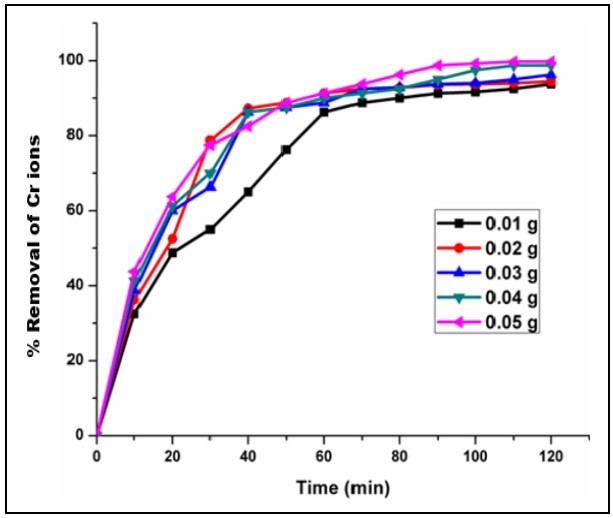

Fig. 2: Effect of adsorbent dosage

3.4 Effect of pH

By increasing the pH from 2 to 8, as well as the adsorbent dosage and metal concentration to 0.05 g and 100 mg l^{-1}, respectively, the impact of pH on the adsorption of Cr (VI) by CLPBC was investigated. The batch experiment was run for varying contact periods, ranging from 10 to 120 minutes. The amount of metal ions adsorbed onto the biosorbent is significantly influenced by the pH of the solution, which also affects the adsorption phenomena (Sun Xining *et al.* 2015). As seen in Fig. 3, there has been an increase in the amount of Cr (VI) adsorbed when the pH of the solution is raised from 2 to 8. pH 7.0 (99.6% of removal) was the ideal pH for the biochar to remove 0.05 g of Cr (VI) per liter. The impact of pH on CLPBC's removal of Cr (VI) is depicted in the figure. In the biochar samples, the carboxylic acid groups of CLPBC organic moiety have proton which moves to the base of the NH_2 sites. The negatively charged dichromate ions on adsorption, will get adsorbed over the ammonium (NH_2) sites through electrostatic attraction. While the ionized form (CrO_4^{2-}) is

preferentially adsorbed at higher pH values, the molecular form ($HCrO_4^-$) is adsorbed largely at lower pH values. Comparable research on the adsorption of lead and cadmium revealed that binding sites start to deprotonate at higher pH levels (above the isoelectric point, or pH 3.0), which makes alternative functional groups available for positively charged metal binding. The fact that an ideal quantity of Cr (VI) was adsorbed at pH 7, which is the natural pH of nearly all natural water bodies, highlights the importance of employing biochar as an adsorbent (Ranganathan and Shreedevi, 2011).

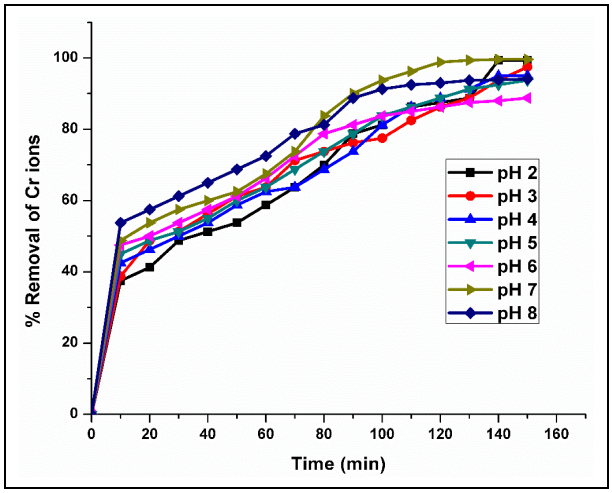

Fig. 3: Effect of pH

3.5 Adsorption Isotherms

3.5.1 Langmuir Isotherm

The sorption data for CLPBC have been subjected to different sorption isotherms, namely, Langmuir, Freundlich, and Temkin. The Langmuir isotherm and the equilibrium values for Cr (VI) at 25 °C, over the concentration range of 50 to 250 mg l^{-1} have been correlated. The Langmuir isotherm is applicable for monomolecular layer adsorption and has been effectively used to get the highest possible adsorption capacity. Langmuir isotherm explains that maximum ion exchange spends on the adsorbate molecule monolayer saturation level on the adsorbent surface (Pragathiswaran *et al.* 2013). There is no adsorbate molecule transmigration on the surface plane, and the energy of ion exchange is constant. Table 2 displays the Langmuir constants, q_m and b, which were calculated from the plot's slope and intercept. Figures 4(a), 4(b), and 4(c) show R^2 values ranging from 0.997 to 0.999, indicating that the Langmuir isotherm offers a satisfactory fit to the isotherm data. The results of this experiment indicate that the adsorption of Cr (VI) onto CLPBC is advantageous at the temperature examined, with the value of R_L determined to be between 0.824 and 0.001 at 30 °C.

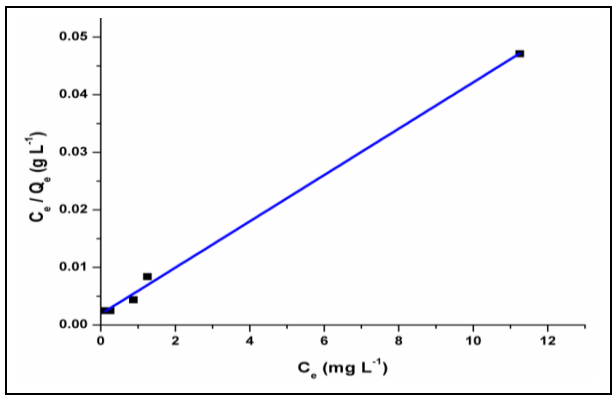

Fig. 4(a): Langmuir isotherm for different concentrations

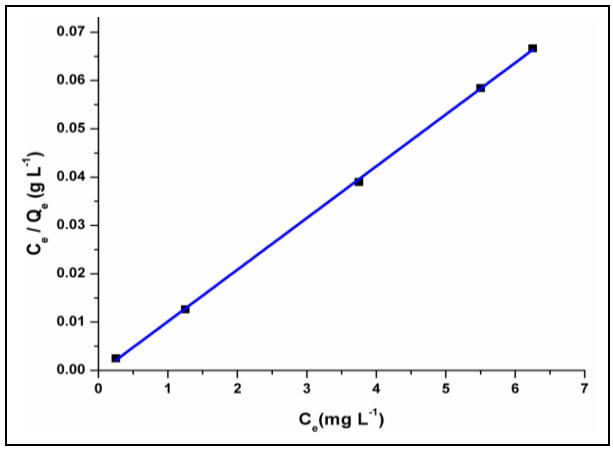

Fig. 4(b): Langmuir isotherm for different dosages

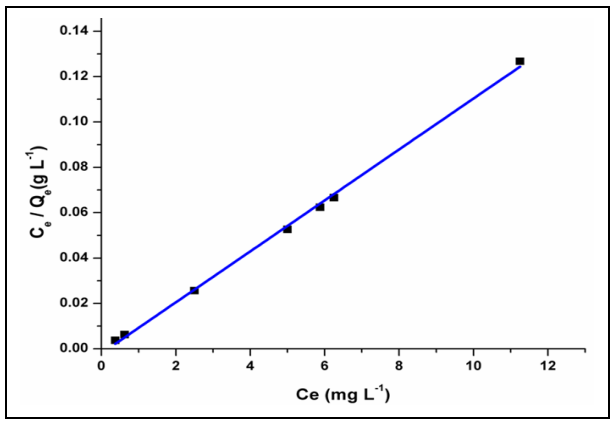

Fig. 4(c): Langmuir isotherm for different pH values

3.5.2 Freundlich Isotherm

Freundlich isotherm explains adsorption onto a heterogeneous surface through a multilayer adsorption mechanism (Sukumar *et al.* 2014). Table 2 summarizes all the Freundlich parameters, together with correlation coefficients (R^2.). The obtained values of n ($0.1<1/n<1$) indicated a higher adsorbent ability of Cr (VI) under study. In this investigation, n values obtained were discovered to be 0.3 for concentration, 0.02 for dosage,

and 0.01 for pH. The R^2 values (between 0.77 and 0.865) of Freundlich isotherm (Fig. 5 (a), 5 (b) and 5 (c)) were found to be lower than the values of Langmuir isotherm.

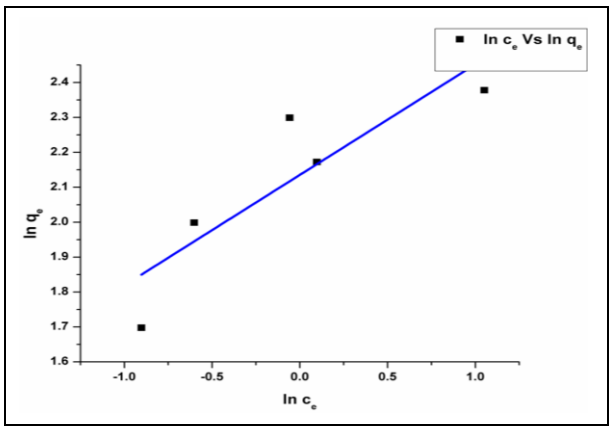

Fig. 5(a): Freundlich isotherm of concentration

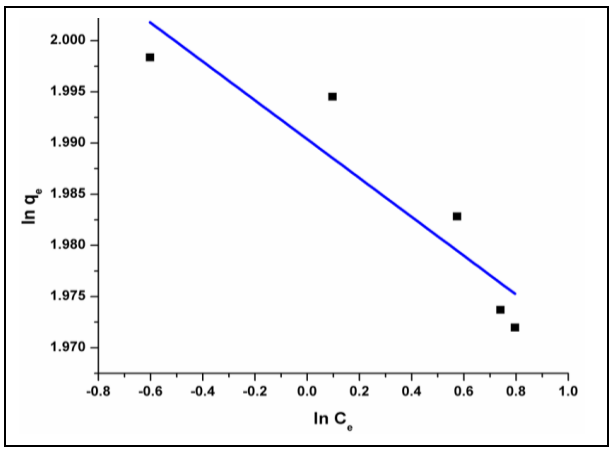

Fig. 5(b): Freundlich isotherm of dosage

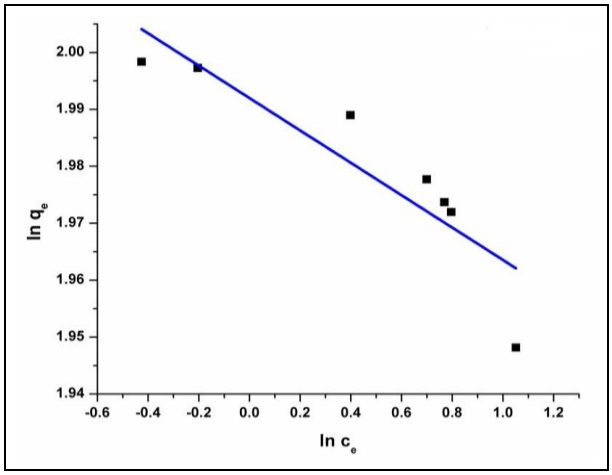

Fig. 5(c): Freundlich isotherm of pH

3.5.3 Temkin Isotherm

Temkin isotherm takes into account the adsorbent-adsorbate interactions on adsorption isotherms. It is predicated on the idea that adsorbate adsorption is equally distributed and that the heat of adsorption of all molecules in the layer reduces linearly with the coverage of molecules as a result of adsorbate-adsorbate repulsions (Raffiea *et al.* 2012). Plotting q_e against ln C_e allowed for the determination of Temkin constants. The values of constant A, which corresponds to the maximal binding energy, and constant B, which is related to the heat of adsorption, are provided in Table 2. The R^2 values ranged between 0.82 to 0.86 of the Temkin isotherm (Fig 6 (a), 6 (b), and 6 (c)) and the values were lower than that obtained for the Langmuir isotherm. Therefore, this isotherm was not also useful for studying the adsorption of Cr (VI) ions over CLPBC.

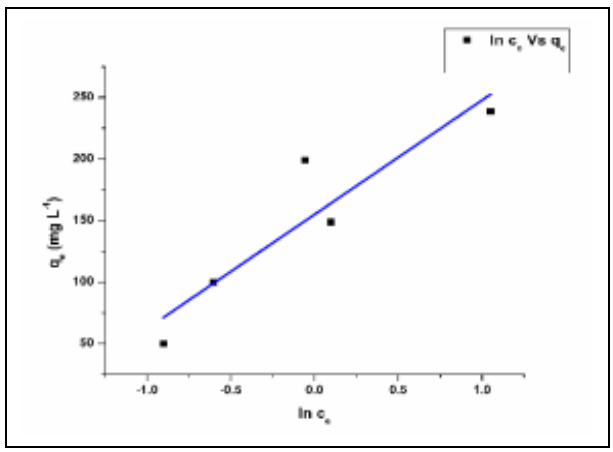

Fig. 6 (a): Temkin isotherm of concentration

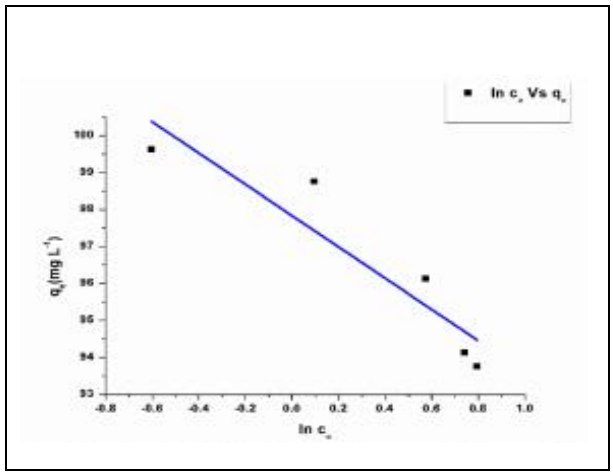

Fig. 6 (b): Temkin isotherm of dosage

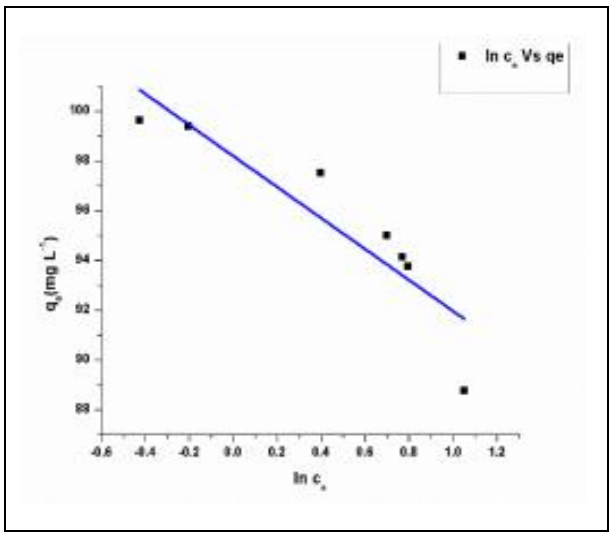

Fig. 6 (c): Temkin isotherm of pH

It is concluded that Langmuir isotherm model befits the equilibrium data followed by the Temkin and Freundlich isotherm models.

3.6 Kinetic models

3.6.1 Pseudo-first-order

The kinetics of Cr (VI) adsorption on the CLPBC was analyzed using pseudo-first-order and pseudo-second-order kinetic models. This pseudo-first-order kinetic model explains that the rate of change of solute uptake with time is directly proportional to the difference in saturation concentration and the amount of solid uptake with time (Ofomaja, 2008). The plot of log ($q_e - q_t$) *vs.* t gives a straight line, where, q_e and q_t are the amounts of chromium adsorbed at equilibrium and at contact time, t. From the slope and intercept of the plot, the adsorption rate constant and equilibrium adsorption capacity were calculated. The conformity between experimental data and the model-predicted values was expressed by the correlation coefficients (R^2 values). Table 3 shows the pseudo-first-order constants, q_e and k_1, along with the corresponding correlation coefficients. The graph (Fig 7 (a), 7 (b), and 7 (c)) and statistical report in Table 3 suggest that the pseudo-first-order model is not suitable for the removal of chromium by CLPBC.

Table 2: Langmuir, Freundlich, and Temkin isotherm constants for chromium ion adsorption by KOH-activated *Citrus limetta* peel

	Langmuir isotherm			Freundlich isotherm			Temkin Isotherm		
	Q_{max}	B	R^2	K_f	N	R^2	A	B	R^2
	(mg/g)	(L/mg)		(mg/g)	(L/mg)	(L/g)	(J/mol)		
Concentration	248.494	2.096	0.9977	136.625	0.3164	0.7709	5.3105	92.8036	0.8540
pH	97.321	86.368	0.9999	98.7678	0.00727	0.7930	1.24	1.655	0.7959
Dosage	98.654	352.98	0.9999	99.0164	0.00468	0.9187	8.07	1.07	0.9195

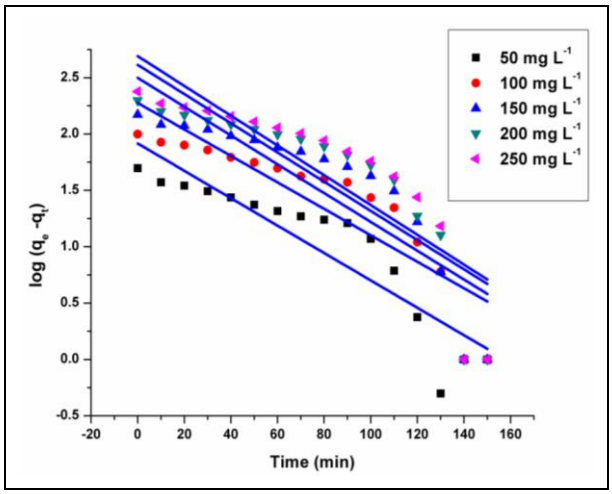

Fig. 7(a): Pseudo-first-order kinetic model for concentration

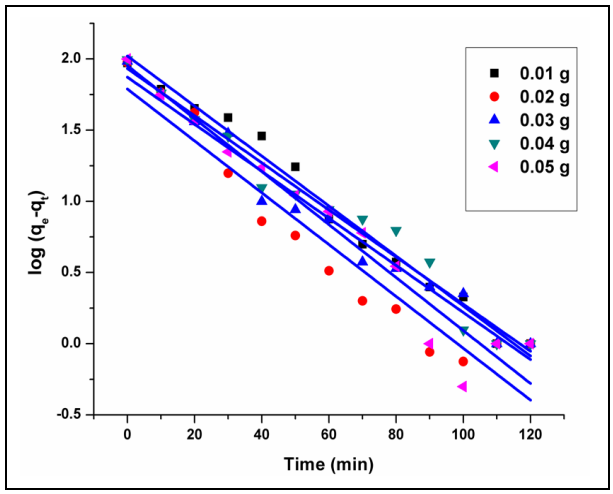

Fig. 7(b): Pseudo-first-order kinetic model for dosage

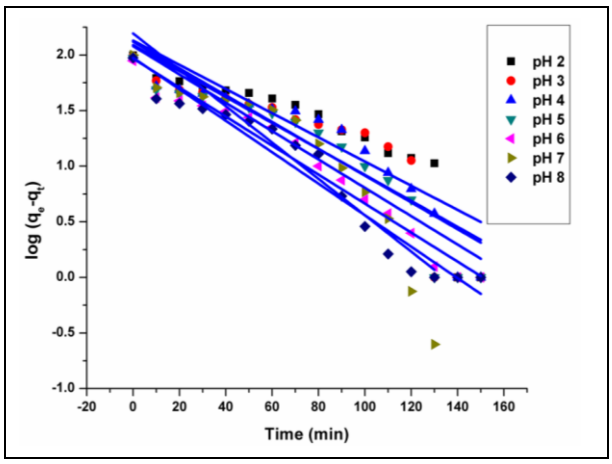

Fig. 7(c): Pseudo-first-order kinetic model for dosage

3.6.2 Pseudo-second-order

The pseudo-second-order model is based on the rate-limiting step which is chemical sorption or chemisorption involving valence forces through exchange of electrons between sorbent and sorbate (Vidhya *et al.* 2023). The figure shows the pseudo-second-order plot for the adsorption of chromium using CLPBC at different initial concentrations. The plot of t/q_t *vs.* t gives a linear relationship from which k_2 and q_e are determined respectively from the intercept and slope of the plots (Fig. 8 (a), 8 (b), and 8 (c)). Table 3 shows that the R^2 values are higher than the values of the pseudo-first-order kinetic model. The adsorption of chromium by CLPBC follows the pseudo-second-order kinetic model.

Table 3: Biosorption kinetics for Cr (VI) on *Citrus limetta* peel biochar

Conc.(ppm)	Q_e (Expt.) mg/g	Pseudo-first order			Pseudo -second order		
		q (Calc.) mg/g	K_1 1/min	R^2	q (Calc.)mg/g	K_2 (g/mg/min)	R^2
50	49.875	82.63235	-0.028	0.824957	64.9762	0.0005	0.949664
100	99.75	188.8648	-152.668	0.778538	157.3108	0.0003	0.965408
150	148.75	315.3544	-0.02944	0.758258	237.9065	0.00014	0.93733
200	199.125	411.5471	-0.02985	0.736461	277.6309	0.00011	0.924565
250	238.75	491.7369	-0.03043	0.730324	324.8230	0.00011	0.934422

Note: Triplicate experiments were carried out and the mean values were reported

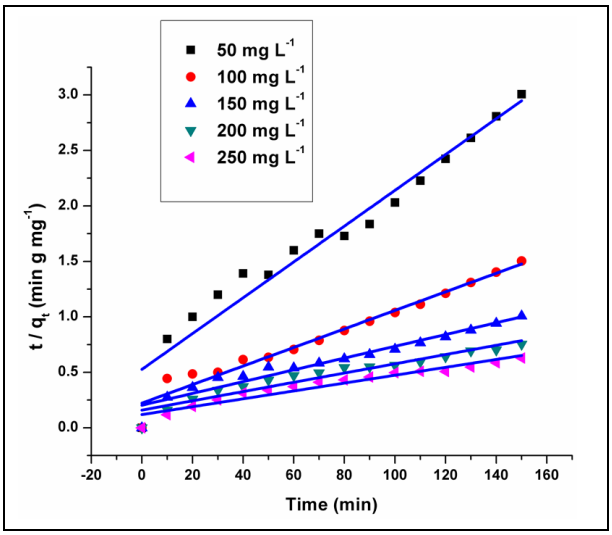

Fig. 8(a): Pseudo-second-order kinetic model for concentration

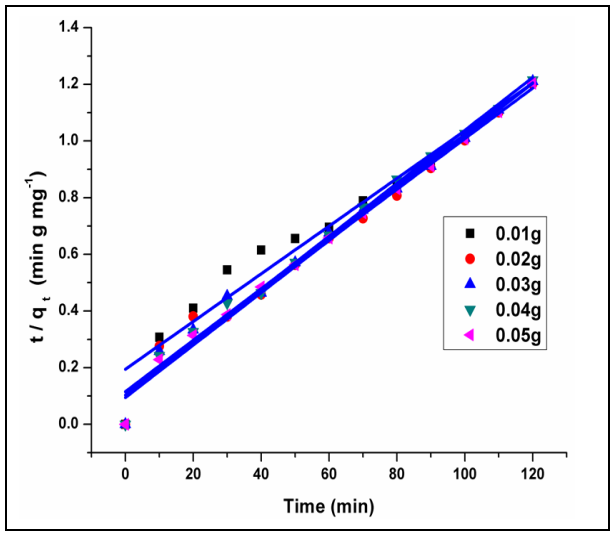

Fig. 8(b): Pseudo-second-order kinetic model for dosage

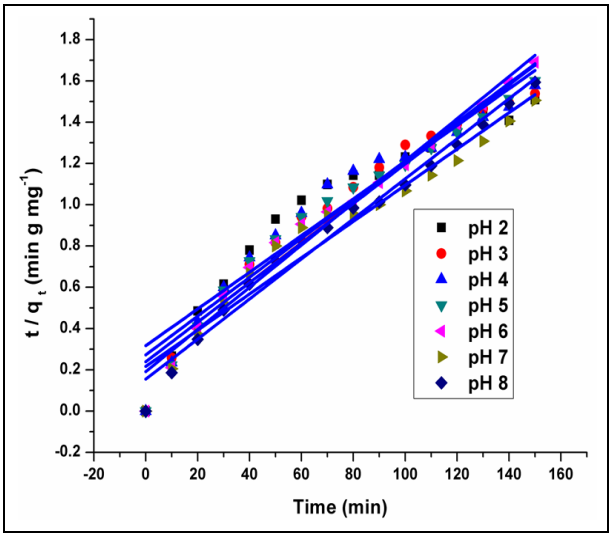

Fig. 8(c): Pseudo-second-order kinetic model for dosage

1.7 Fourier Transform Infrared Analysis (FT-IR)

The FT-IR spectra of KOH-activated *Citrus limetta* peel biochar before and after the sorption of chromium were used to determine the vibration frequency changes of the functional groups in the adsorbents. The spectra of adsorbents were measured within the rangeof 4000-400 cm^{-1} wave numbers (Fig. 9).

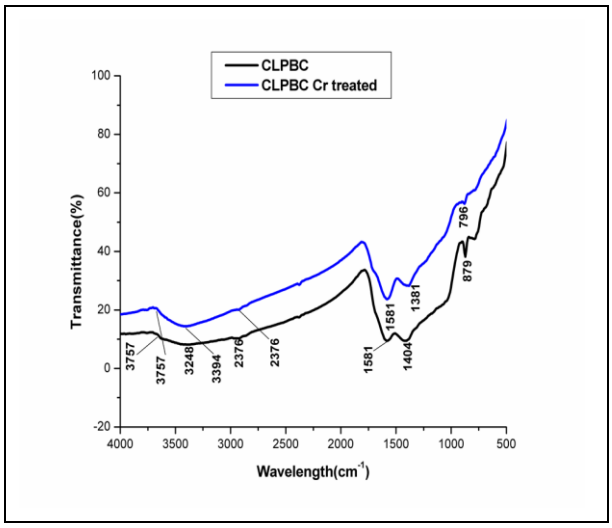

Fig. 9: FTIR of KOH-activated *Citrus limetta* peel biochar before and after sorption of chromium

For every adsorbent, both before and after adsorption, the spectra were plotted on the transmittance axis using the same scale. Numerous adsorption peaks can be seen in the FT-IR spectra of the adsorbents, showing their complex character. The essential peaks of the adsorbents before and after Cr (VI) are shown in Table 4.

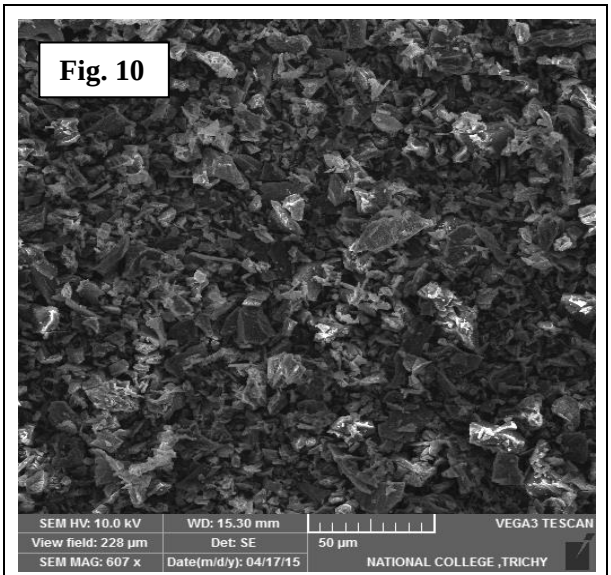

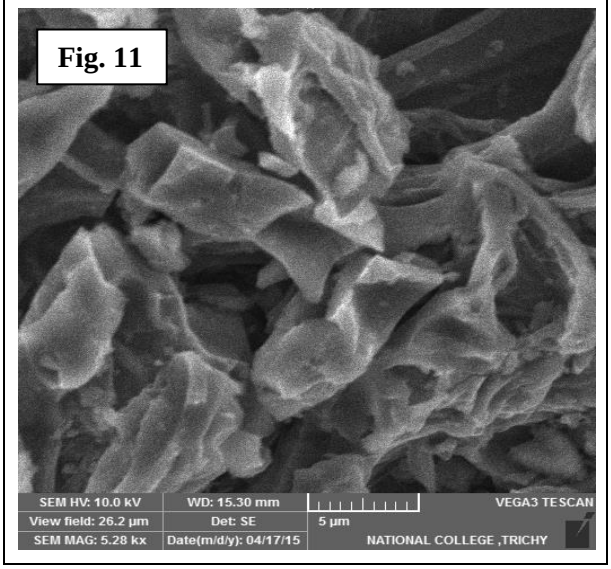

Fig. 10 & Fig. 11: SEM Micrographs of *Citrus limetta* peel biochar before and after Cr (VI) adsorption, respectively

In this study, the FT-IR spectra of metal-loaded and unloaded *Citrus limetta* peel biochar display several adsorption peaks, which are expected for biochar samples. The frequency at 3757 cm^{-1} indicates the OH stretch vibration with the presence of hydroxo complexes. The same frequency is also observed after adsorption of chromium. The broadness of the vibration frequencies indicates inter and intra-molecular hydrogen bonding in the biochar (Shin *et al.* 2012). A peak observed at 3248 cm^{-1} was due to the stretching vibrations of O–H bonds. The increase of the frequency (3394 cm^{-1}) was observed in the after-adsorptionof biosorbents implicating the presence of hydrogen-bonded alcohols. Apart from this, a characteristic peak at

2924 cm^{-1} was found both before and after adsorption. It represents the O–H stretching confirming the presence of phenols. At 1581 cm^{-1} CO stretching vibration is seen in both the adsorption showing the presence of carboxylic acids. It is found that after Cr (VI) adsorption, aminor shift in the peak from 1404 to 1381 cm^{-1} was observed indicating the presence of aliphatic aldehydes. A C-H rocking vibration is identified. The decrease in the peak from 879 to 796 cm^{-1} shows the bonding of CO_2 scissor vibrations explaining the presence of carboxylic acid salts in the adsorption process.

1.8 SEM and EDAX Analysis

Morphological structures of the *Citrus limetta* peel biochar as revealed by Scanning Electron Microscopy (SEM) before and after chromium (VI) adsorption are shown in Fig. 10 and Fig. 11.

The biochar particles before adsorption are scattered and porous (Fig. 10). The porosity of biochar after adsorption is less (Fig. 11) as compared to before adsorption (Fig. 10), which indicates the adsorption of chromium in the pores of the sample that are irregular and its porous nature facilitated the adsorption (Yusof and Malek, 2009). After adsorption, the bio-adsorbent and chromium were coupled as represented in Fig.11. The results are consistent with previous studies that reported the changes in the nature of the adsorbent after the adsorption process.

Furthermore, the EDAX spectra of the selected zoneof biochar before adsorption and after adsorption were analyzed to find the chemical constituents in the biochar sample (Figures 12 and 13), which confirmed the adsorption of Cr (VI) ions. EDAX analysis also confirmed the presence of potassium, calcium, and phosphorus peaks in both control and test samples.

Table 4: Variation in vibration frequencies of *Citrus limetta* peel biochar and corresponding functional groups, before and afteradsorption

Citrus limetta peel biocharFrequeny (cm^1)	Chromium adsorbed *Citrus limetta* peel biochar frequency (cm^{-1})	Type of vibration	Functional group
3757	3757	O–H stretch	hydroxo complexes M -OH
3248	3394	O–H stretch, H –bonded	hydroxy bonded alcohols, phenols
2924	2924	O-H stretch	phenols
2376	2376	COOH	amino acids
1581	1581	CO_2^- stretching	carboxylic acids
1404	1381	C-H rocking vibration	aliphatic aldehydes
796	879	CO scissor vibration	carboxylic acid salts

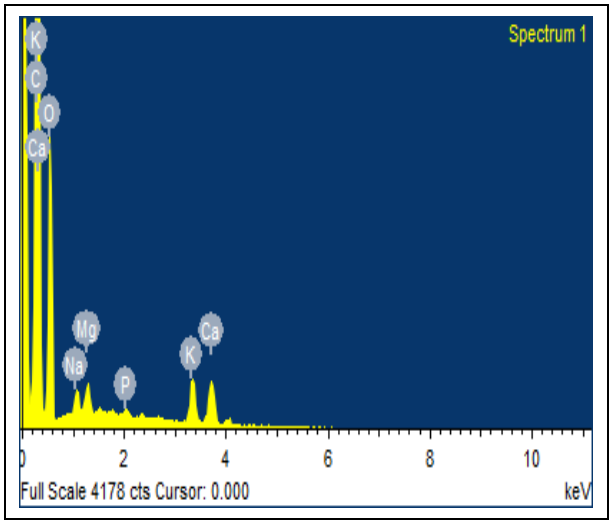

Fig. 12. EDAX spectrum of *Citrus limetta* peel biochar before Cr (VI) adsorption

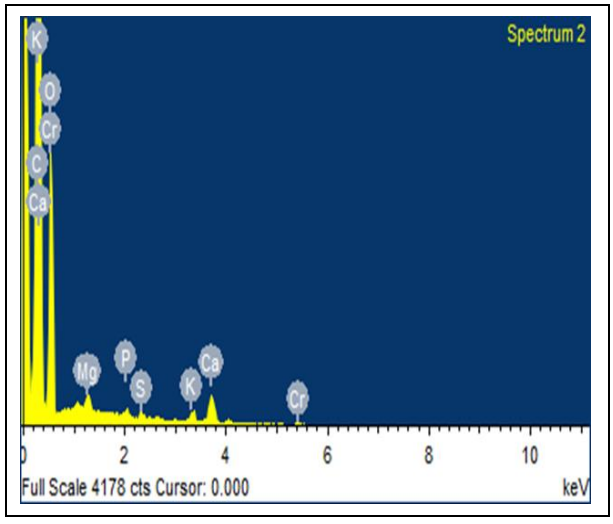

Fig. 13: EDAX spectrum of *Citrus limetta* peel biochar after Cr (VI) adsorption

4. CONCLUSION

KOH-activated *Citrus limetta* (sweet-lime) peel biochar was evaluated for the elimination of Cr (VI) from aqueous solutions. The removal of Cr (VI) was found to be dependent on different parameters such as adsorbent dose, contact time, pH, and initial concentration. The bio-adsorbent, *Citrus limetta* peel biochar exhibited an effective removal of 99.8% Cr (VI) at a concentration of 100 ppm, pH 7, and at the time interval between 0 and 150 min. Second-order kinetics of adsorption of Cr (VI) was noticed with *Citrus limetta* peel biochar. The data on adsorption befittingly match the Langmuir isotherm. The physical structure analyses like SEM and FT-IR revealed distinct phases with greater numbers of pores or sites available for adsorption by the biochar. Higher sorption capacity indicates that *Citrus limetta* peel biochar can effectively and economically be used for the treatment of Cr (VI) ion adsorption from industrial effluents.

ACKNOWLEDGEMENTS

The authors express their gratitude to the Hindusthan College of Engineering and Technology management and principal for their assistance in completing the project successfully. The author is grateful to the Departments of Environmental Science in PSG College of Arts and Science, and Tamil Nadu Agricultural University, both located in Coimbatore, India, and the Department of Chemistry, National College, Tiruchirappalli, India, for providing facilities and extending cordial gestures during this study.

FUNDING

This research received no specific grant from any funding agency in the public, commercial, or not-for-profit sectors.

CONFLICTS OF INTEREST

The authors declare that there is no conflict of interest.

COPYRIGHT

REFERENCES

Attia, A. A., Khader, S. A. and Elkholy, S. A., Adsorption of Chromium ion (VI) by acid activated carbon, *Brazilian J. Chem. Engg*., 27, 183-193 (2010). https://doi.org/10.1590/S0104-66322010000100016

Babu, B. V. and Gupta, S, Adsorption of Cr(VI) using activated neem leaves, *Kinetic Studies*, 14, 85-92 (2008). https://doi.org/10.1007/s10450-007-9057-x

Bello, Olugbenga, S., Oluwole, A. O. and Victor, O. N., Fly ash: An alternative to powdered activated carbon for the removal of eosin dye from aqueous solutions, *Bull. Chem. Soc. Ethiop*., 27, 191-204 (2013). https://doi.org/10.4314/bcse.v27i2.4

Demirbas, E., Kobya, M., Senturk, E. and Ozkan, T., Adsorption kinetics for the removal of chromium (VI) from aqueous solutions on the activated carbons prepared from agricultural wastes, *Water SA*, 30, 533-539 (2004). https://doi.org/10.4314/wsa.v30i4.5106

Dhungana, T. P. and Yadav, P. N., Determination of chromium in tannery effluent and study of adsorption of Cr(VI) on sawdust and charcoal from sugarcane bagasses, *J. Nepal Chem. Soc*., 23, 120-125 (2008). https://doi.org/10.3126/jncs.v23i0.2102

Erdem, E., Karapinar, N. and Donat, R., The removal of heavy metal cations by natural zeolites, *J. Colloid. and Interface Sci*., 280, 309–314 (2004). https://doi.org/10.1016/j.jcis.2004.08.028

Jabari, M., Aqra, F., Shahin, S. and Khatib, S, Monitoring chromium content in tannery waste water, *J. Argentine Chem. Soc*., 97, 77-87 (2009).

Jeyagowri, B. and Yamuna, R. T., A cost effective green biosorbent *Simarouba glauca* seed shell for removal of rhodamine B from aqueous solutions, *Asian Jr of Chemistry*, 27(6), 2288-2294 (2015). https://doi.org/10.14233/ajchem.2015.18764

Khan, A., Tabrez, M. N., Imran, A. and Ajeet, K., Removal of chromium (VI) from aqueous solution using guar gum–nano zinc oxide biocomposite adsorbent, *Arabian J. Chem*., 19, 1878-5352(2013). http://dx.doi.org/10.1016/j.arabjc.2013.08.019

Kucic, D., Marinko, M. and Felicita, B., Ammonium adsorption on natural zeolite (clinoptilolite): adsorption isotherms and kinetics modeling, *The Holistic Approach to Environ.*, 2, 145-158 (2012).

Nevine, K. A., Removal of reactive dye from aqueous solutions by adsorption onto activated carbons prepared from sugar-cane bagasse pith, *Water Treat. Soln. and Desalination*, 223, 152-161 (2008). https://doi.org/10.1016/j.desal.2007.01.203

Ofomaja, A. E., Sorptive removal of methylene blue from aqueous solution using palm kernel fibre: effect of fibre dose, *Biochem. Eng. J*., 40, 8-18 (2008). https://doi.org/10.1016/j.bej.2007.11.028

Owlad, M., Aroua, M. K., Daud, W. A. and Baroutian, S., Removal of hexavalent chromium- contaminated water and wastewater, A review, *Water Air and Soil pollution*, 200(1), 59-77 (2008). https://doi.org/10.1007/s11270-008-9893-7

Pragathiswaran, C., Sibi, S. and Sivanesan, P., Comparison studies of various adsorption isotherms for *Aloe vera* adsorbent, *Int. J. Res. Pharm. Chem*., 3, 40-45 (2013).

Pradeeba, S. J. and Sampath, K., Synthesis and Characterization of Poly(azomethine)/ZnO Nanocomposite Towards Photocatalytic Degradation of Methylene Blue, Malachite Green, and Bismarck Brown, *J. Dyn. Sys., Meas., Control*., 141(5), 051001, (2019). https://doi.org/10.1115/1.4042090

Raffiea, J. B., Palanisamy, P. N. and Sivakumar, P., Adsorption of basic dyes from synthetic textile effluent by activated carbon prepared from *Thevetia peruviana*, *Indian J. Chem. Technol*., 19, 311-321 (2012).

Ramzy, B. N., Ahmad, R. B., Hermine, R. Z., Madelyn, N. M. and Kamal, M. K., Biosorption of lead and cadmium using marine algae, *Chem. Ecol*., 27(6), 579-594 (2011). https://doi.org/10.1080/ 02757540.2011.607439

Ranganathan, K. and Shreedevi, D., Studies on feasibility of reverse osmosis (membrane) technology for treatment of tannery wastewater, *J. Environ. Protect*., 2, 37-46 (2011). https://doi.org/10.4236/jep.2011.21004

Shah, M. A. and Tokeer, A., Principles of Nanoscience and Nanotechnology, Narosa Publishing House, New Delhi (2013).

Shenbagavalli, S. and Mahimairaja, S., Production and characterization of biochar from different biological Wastes, *Int. J. Plant and Agric. Sci*., 12, 2231-4490 (2014).

Shin, M. N., Shim, J., You, Y., Myung, H., Bang, K. S., Cho, M., Kamala Kannan, S. and Oh, B. T., Characterization of lead resistant endophytic *Bacillus* sp. MN3-4 and its potential for promoting lead accumulation in metal hyperaccumulator Alnus firma, *J. Hazard. Mater*., 199-200, 314-320 (2012). https://doi.org/10.1016/j.jhazmat.2011.11.010

Sukumar, C., Janaki, V., Seralathan, K. K. and Shanthi, V., Biosorption of chromium (VI) using *Bacillus subtilis* SS-1 isolated from soil samples of electroplating industry, *Clean Technol. Envir*., 16, 405-413 (2014). https://doi.org/10.1007/s10098-013-0636-0

Sun, X., Mi, J., Zhang, Z. and Zhang, Z., Biosorption of hexavalent chromium from aqueous medium with the antibiotic residue, *Adv. J. Food Sci. Technol*., 7, 120-128 (2015). https://doi.org/10.19026/ajfst.7.1279

Vargas, C., Pedro, F. B., Jesus, A. and Elianna, C., Cr(VI) removal by compost, *Bio Resources*, 7, 2711-2727 (2012).

Vidhya, L., Vinodha, S., Pradeeba, S. J., Jeyagowri, B., Nirmaladevi, V. and Nithiya, N., Adsorption and Kinetic Studies on Sequestering Effect of Porous Biodegradable Biochar Obtained from Pig-Bone on Hexavalent Chromium from Aqueous Solution, *Nature Envir. and Pollut. Techno.*, 22(2), 681-690 (2023). https://doi.org/10.46488/NEPT.2023.v22i02.01

Vikrant, S. and Pant, K. K., Removal of chromium from industrial waste by using eucalyptus bark, *Bioresource Technol*., 97, 15-20 (2006). https://doi.org/10.1016/j.biortech.2005.02.010

Wanna, S. and Pairat, K., Cadmium ion removal using biosorbents derived from fruit peel wastes, *Songklanakarin J. Sci. Technol*., 31, 547-554 (2009).

Yang, Y., Lin, X., Wei, B., Zhao, Y and Wang, J., Evaluation of adsorption potential of bamboo biochar for metal-complex dye: equilibrium, kinetics and artificial neural network modeling, *Int. J. Environ. Sci. Technol*., (2014). https://doi.org/10.1007/s13762-013-0306-0

Yusof, A. and Malek, N., Removal of Cr (VI) and As (V) from aqueous solutions by HDTMA-modified zeolite, *J. Hazardous Mat*., 162, 1019-1024 (2009). https://doi.org/10.1016/j.jhazmat.2008.05.134